



## Recycling studies based on two-dimensional visible light measurements and Monte-Carlo simulation in mirror and helical systems

Y. Nakashima<sup>a,\*</sup>, Y. Higashizono<sup>a</sup>, H. Kawano<sup>a</sup>, N. Nishino<sup>b</sup>, S. Kobayashi<sup>c</sup>, T. Mizuuchi<sup>c</sup>, M. Shoji<sup>d</sup>, K. Nagasaki<sup>c</sup>, H. Okada<sup>c</sup>, F. Sano<sup>c</sup>, K. Kondo<sup>e</sup>, Y. Yoneda<sup>a</sup>, R. Yonenaga<sup>a</sup>, M. Yoshikawa<sup>a</sup>, T. Imai<sup>a</sup>

<sup>a</sup> Plasma Research Center, University of Tsukuba, 1-1-1 Tennoudai, Tsukuba, Ibaraki 305-8577, Japan

<sup>b</sup> Graduate School of Engineering, Hiroshima University, Hiroshima 739-8527, Japan

<sup>c</sup> Institute of Advanced Energy, Kyoto University, Gokasho, Uji 611-0011, Japan

<sup>d</sup> National Institute for Fusion Science, Toki, Gifu 509-5292, Japan

<sup>e</sup> Graduate School of Energy Science, Kyoto University, Gokasho, Uji 611-0011, Japan

### ARTICLE INFO

#### PACS:

52.25.Ya

52.40.Hf

52.55.Jd

52.65.Pp

### ABSTRACT

Analysis of neutral particle behavior in the GAMMA 10 tandem mirror with open magnetic field and the Heliotron J device with non-axisymmetric plasma confining system is described based on the results of Monte-Carlo neutral transport simulation. Three-dimensional (3-D) Monte-Carlo code DEGAS was applied to both devices in order to investigate precisely the spatial distribution of neutral particle density. In GAMMA 10, a detailed structure of inner components of the central-cell is modeled in the simulation space. In Heliotron J, a carbon limiter inserted into the plasma for investigation of plasma-material interactions is also modeled in addition to the helically twisted vacuum vessel and plasma. In both devices, 2-D images of light-emission from the plasma captured with CCD cameras near the limiters are compared with the simulation results and a good agreement between experiment and simulation is recognized. Comparison of the decay length in the emissivity of  $H\alpha/D\alpha$  line-emission also showed that neutral transport in SOL region plays a significant influence on the emission profile.

© 2009 Elsevier B.V. All rights reserved.

### 1. Introduction

Investigation of recycling is one of the important subjects for controlling plasma in magnetically plasma confining devices. Analysis of neutral transport phenomena also gives us useful information on plasma-material interactions as well as edge plasma behavior. In particular, the neutral transport analysis in non-axisymmetric plasma confining systems, such as helical systems and mirror systems with minimum-B configuration, becomes much complicated, since the plasma and the wall are configured in three-dimensional (3-D) structure. 3-D Monte-Carlo simulation of the neutral transport is an indispensable method in order to solve this difficulty. Neutral transport studies in 3-D geometry by using DEGAS Monte-Carlo code [1,2] have been carried out in the GAMMA 10 tandem mirror device [3,4], the helical device LHD [5] and Heliotron J [6,7].

Visible image diagnostic using high-speed camera is also a powerful method for visualizing the behavior of edge plasma behavior [8]. In GAMMA 10 and Heliotron J devices, high-speed cameras have been installed and measurements of 2-D visible images of

plasma light-emission were performed and the distinctive behavior of each plasma was observed [9,10].

In this study neutral particle behavior due to the limiter recycling is investigated in the GAMMA 10 central-cell and Heliotron J plasmas based on the 3-D Monte-Carlo simulation of neutrals. In both devices, neutral transport simulation corresponding to the 2-D images of light-emission near the limiters is carried out. In this paper a discussion on the influence of localized particle source due to the interaction between plasma and limiter follows a comparison between the experimental results and simulations.

### 2. Experimental setup and simulation model

#### 2.1. GAMMA10 tandem mirror

GAMMA 10 consists of an axisymmetric central-mirror cell, anchor-cells with minimum-B configuration using baseball coils, and plug/barrier cells with axisymmetric mirrors [11]. The central-cell 6 m in length and 1 m in diameter is connected to the anchor-cells through the mirror throat regions. Fig. 1(a) shows the schematic view of the central and the anchor-cells of GAMMA 10 together with the diagnostic systems related to this study. A number of  $H\alpha$  line-emission detectors are installed along the machine axis (z-axis) from the central-cell midplane ( $z = 0$ ) to the east anchor-

\* Corresponding author.

E-mail address: [nakashma@prc.tsukuba.ac.jp](mailto:nakashma@prc.tsukuba.ac.jp) (Y. Nakashima).

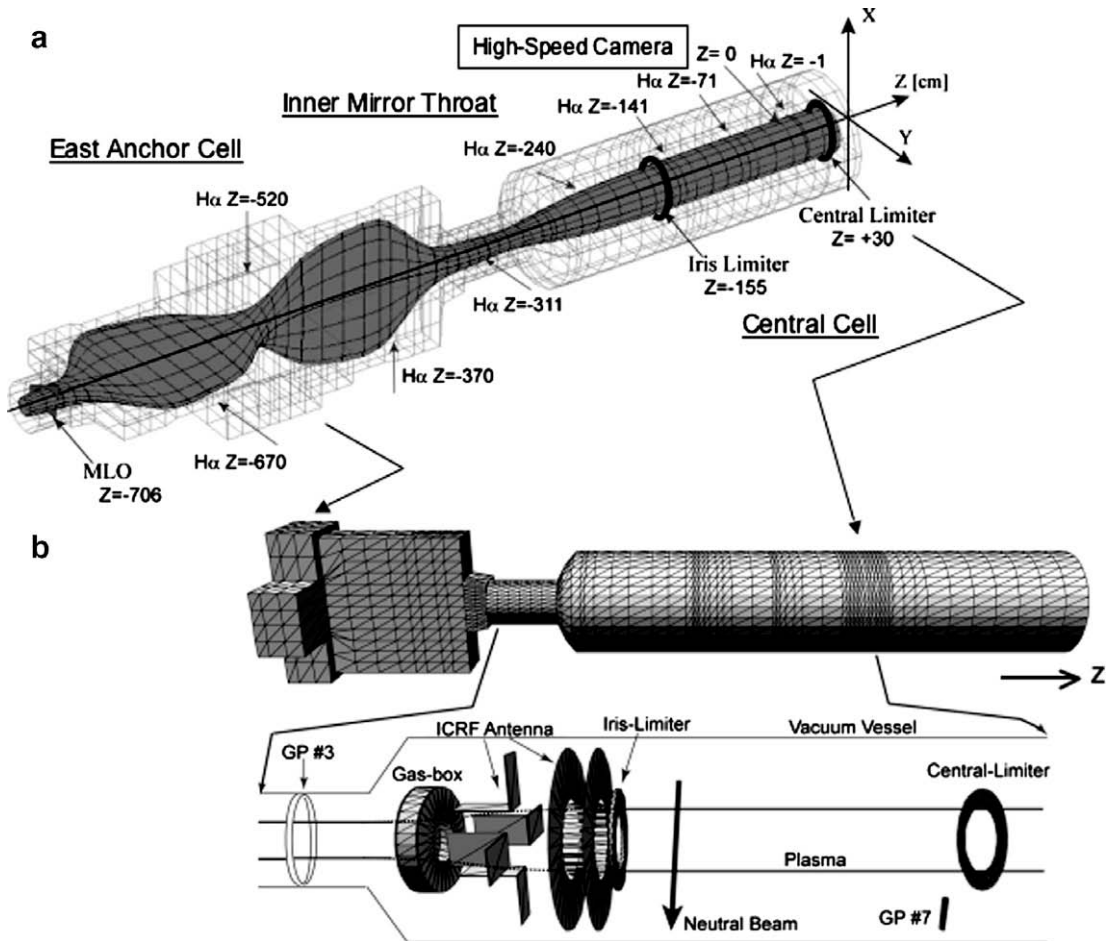


Fig. 1. Experimental setup and mesh model of the GAMMA 10 central-cell. (a) Schematic drawing of the GAMMA 10 central-cell and east anchor-cell together with the location of H $\alpha$  detectors and high-speed camera. (b) Fully 3-dimensional mesh model for DEGAS simulation.

cell ( $-750 \text{ cm} < z < -300 \text{ cm}$ ). A medium-speed CCD camera with the frame rate of 400 fps and  $216 \times 640$  pixels has been installed in front of a horizontal port of the central-cell midplane and the camera monitors the plasma behavior near the central-cell limiter located at  $z = +30 \text{ cm}$ . The camera observes total light or H $\alpha$  line-emission from the plasma using interference filter and it is confirmed that the total light from the limiter mainly comes from H $\alpha$  emission. Fig. 1(b) shows the fully 3-D mesh model of GAMMA 10 central-cell. In this model, interior components, such as limiter, radio frequency (RF) antenna and gas puff are precisely integrated together with the central-cell vacuum vessel. In the simulation, calculation on the assumption of recycling particle source from the limiter is carried out and a comparison to captured 2-D image from the CCD camera.

## 2.2. Heliotron J

In Fig. 2(a), bird's eye view of the Heliotron J plasma and the location of plasma heating system and diagnostics used in the experiment are presented. Heliotron J is the helical axis heliotron device with a helical winding coil of  $L/M = 1/4$ , where  $L$  and  $M$  are the pole number of the helical coil and the helical pitch, respectively [12,13]. In a standard magnetic field configuration, the average major and minor radii of the plasma are 1.2 m and 0.17 m, respectively. The carbon limiter is inserted from the bottom of the vacuum vessel in order to study plasma-material interactions in non-axisymmetric plasmas. The carbon limiter consists of a hemispheric head with 9 cm diameter and a ceramic shaft of

6 cm in diameter. In this experiment, a 70 GHz electron cyclotron heating (ECH) system (70 GHz, 0.4 MW) is mainly used for the plasma production and heating. In Heliotron J, a CCD camera with the frame rate of 250 fps and  $512 \times 480$  pixels is installed and the visible light near the carbon limiter is observed horizontally or vertically. In this experiment, an interference filter with the wavelength of H $\alpha$ /D $\alpha$  line-emission ( $\lambda = 656.3 \text{ nm}$  and 10 nm FWHM) is inserted in front of the camera and the time behavior the D $\alpha$  emission from the plasma is monitored.

The 3-D mesh model covering the whole area of Heliotron J for the DEGAS simulation is shown in Fig. 2(b). In this simulation, 3-D modeling of the carbon limiter is carried out in addition to the plasma and vacuum vessel wall of the Heliotron J in order to study the neutral particle behavior near the limiter in this experiment. The mesh is divided into radially 15 segments and 28 segments in the poloidal cross-section, respectively. The toroidal segmentation is taken into 512 to investigate the toroidal variation of neutral density in detail especially near the limiter. The mesh model of the limiter is divided into 40 segments in azimuthal direction and vertically divided into 34 segments.

## 3. Experiment and simulation results

### 3.1. Simulation results near the GAMMA 10 central-cell limiter and comparison with the visible light measurement

Fig. 3 shows the simulation results under the condition with the recycling particle source is located on the limiter in the GAMMA 10

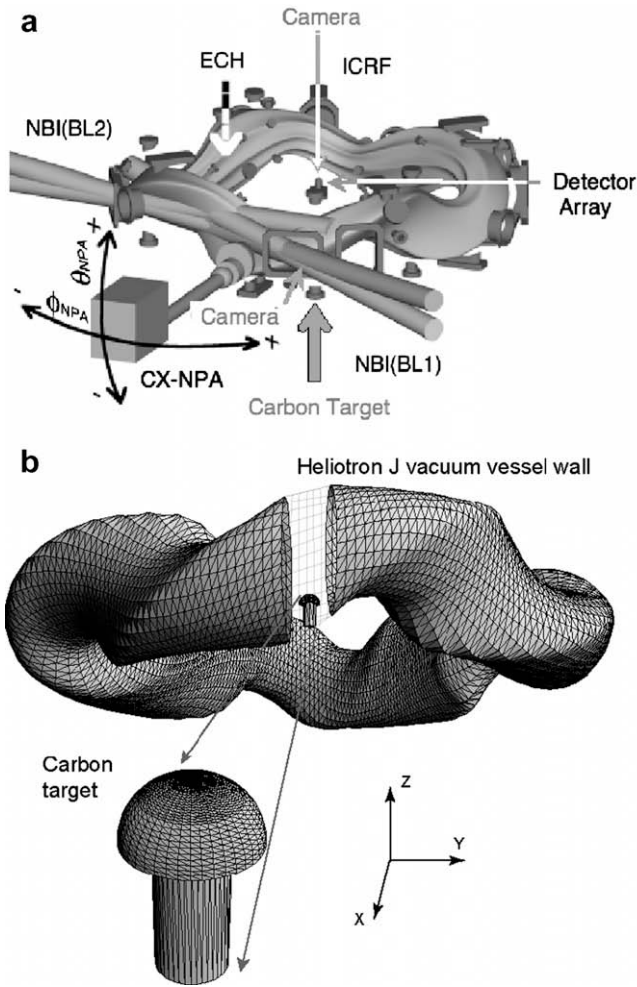


**Fig. 2.** Experimental setup and mesh model of Heliotron J. (a) Schematic view of the Heliotron J vacuum vessel and the location of the plasma heating and diagnostic systems for the experiment. (b) Mesh model of the Heliotron J vacuum vessel, plasma and carbon limiter for the DEGAS simulation.

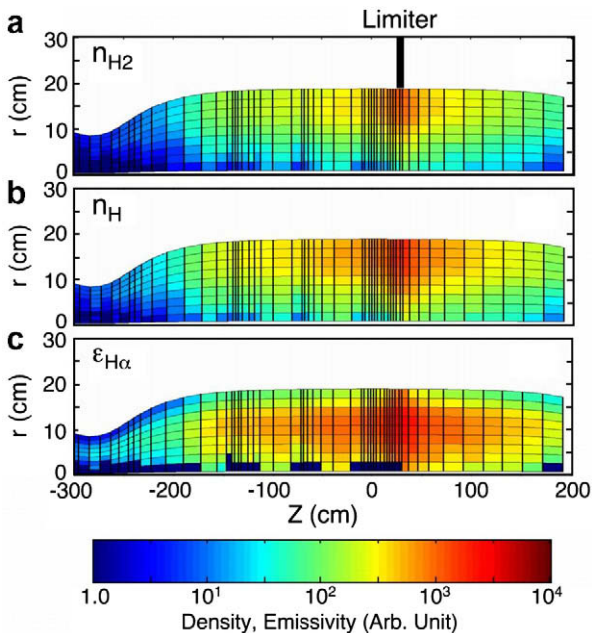


**Fig. 3.** Results of the DEGAS simulation; cross-sectional view of (a) molecular hydrogen density, (b) atomic hydrogen density and (c) emissivity of H $\alpha$  line-emission.

central-cell. In this simulation, under the background plasma parameters based on the experimental data, hydrogen particle is emitted from the inner edge of the limiter (2 cm in width). The simulation result of H $\alpha$  emissivity is averaged in the azimuthal direction, since the particle source is given to be axisymmetric. As shown in Fig. 3(a), hydrogen molecular density becomes maximum just under the limiter and decreases radially toward the plasma center by one order of magnitude. In the plasma edge region, the molecular density decreases along the magnetic field line by one order of magnitude in the distance of more than 1 m from the limiter. Hydrogen atoms, on the other hand, penetrate into the plasma core without any reduction and diffuse wider along the magnetic field line (Fig. 3(b)). The peak position of H $\alpha$  emissivity is located at a few cm inner of the plasma edge as shown in Fig. 3(b). In Fig. 4, calculated 2-D image of H $\alpha$  emission is compared with the measured result of the CCD camera. As shown in Fig. 4(a), the diameter in the visible image of the plasma column is expanded near the limiter which indicates the enhancement of hydrogen recycling due to the limiter–plasma interactions. The simulation result shown in Fig. 4(b) well reproduces this observation result.

3.2. D $\alpha$  emission and neutral behavior near the carbon limiter in Heliotron J

Fig. 5 shows the comparison between the 2-D D $\alpha$  image with high-speed camera and the simulation result in Heliotron J. This simulation is carried out by optimizing the particle source profile on the carbon limiter so as to reproduce the top view of the 2-D image of D $\alpha$  emission obtained by the vertically viewing camera. As shown in the figure, a fairly good agreement is recognized between the simulation and measurement.

In Fig. 6, D $\alpha$  emissivity profile on the vertical cross-section of plasma is shown as a parameter of the plasma density which is artificially varied. This cross-section is made by cutting the plasma along the magnetic axis intersecting the top of the carbon limiter. As shown in the figure, in the density range of actual Heliotron J plasmas ( $1\text{--}2 \times 10^{13} \text{ cm}^{-3}$ ), D $\alpha$  emission profile is found to be enhanced along the magnetic field line (Fig. 6(a and b)). In the lower

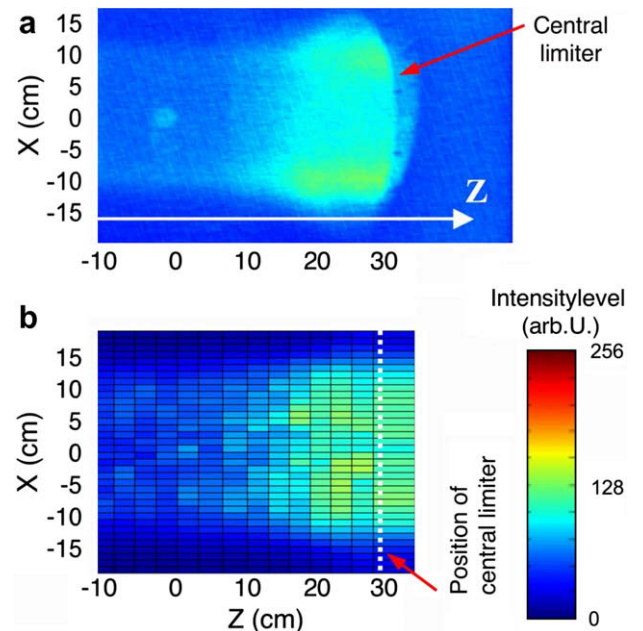


**Fig. 4.** (a) 2-D visible image of the light-emission from the GAMMA 10 plasma by CCD camera. (b) 2-D H $\alpha$  image obtained from the DEGAS simulation.

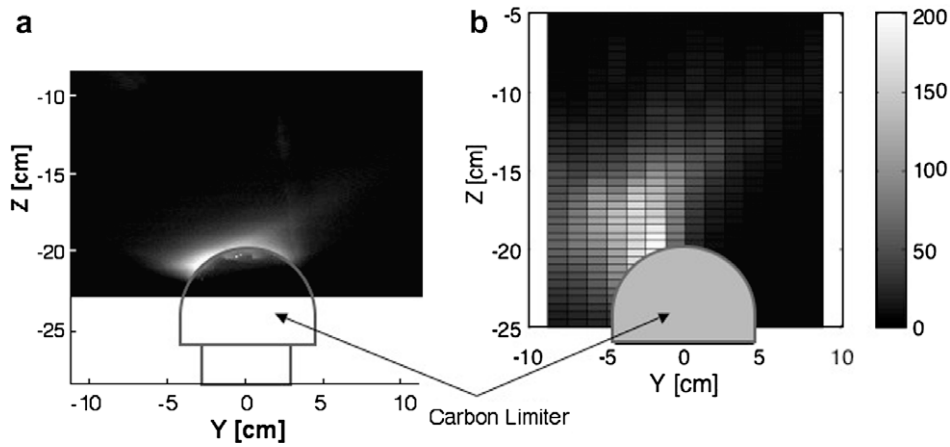


Fig. 5. Comparison between 3D-DEGAS simulation and experiment in Heliotron J. (a) 2-D Dα image of the side view of the carbon limiter. (b) Predicted 2-D image of the Dα intensity near the carbon limiter.

density region such as GAMMA 10 plasmas ( $\sim 2 \times 10^{12} \text{ cm}^{-3}$ ), on the other hand, penetration of Dα emission area toward the plasma core region is recognized and diffusion across the magnetic field line becomes large.

#### 4. Discussion

In order to investigate the common mechanism of neutral particle behavior in both devices, the decay profile of Hα/Dα line-

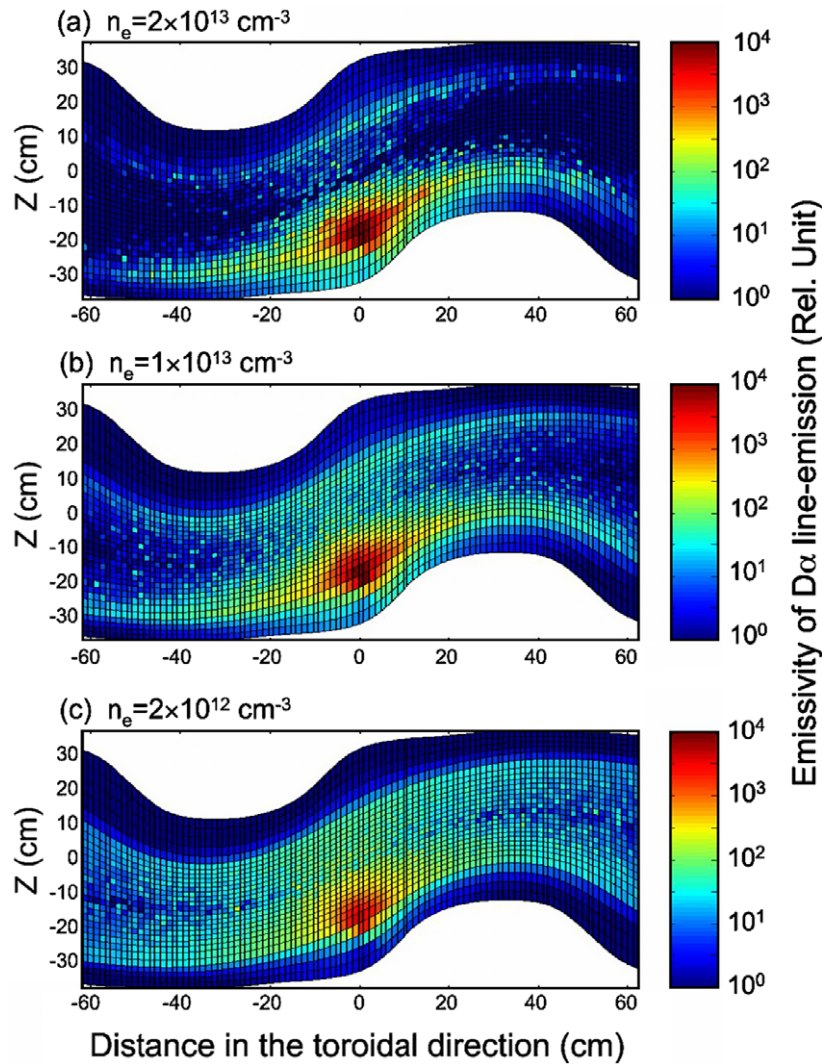


Fig. 6. Cross-section view of Dα emissivity near the carbon limiter predicted from the simulation; (a)  $n_e = 2 \times 10^{13} \text{ cm}^{-3}$ , (b)  $2 \times 10^{13} \text{ cm}^{-3}$ , (c)  $2 \times 10^{12} \text{ cm}^{-3}$ .

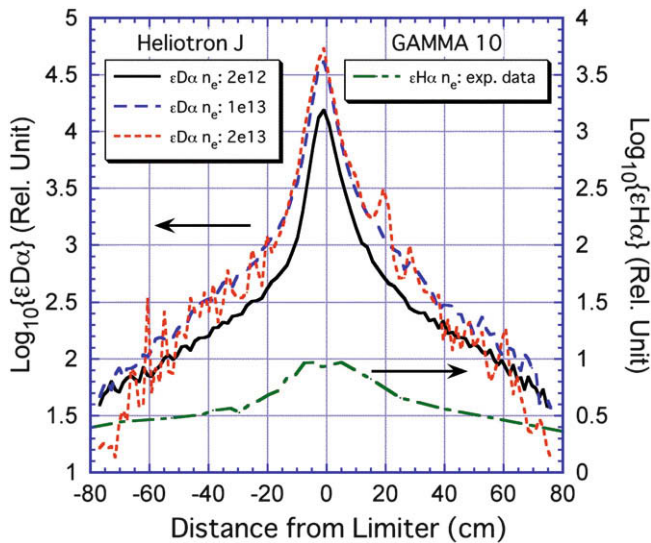


Fig. 7. Comparison of the decay length of  $H\alpha/D\alpha$  emissivity along the magnetic field line obtained from the simulation.

emission was evaluated from the simulation results. In Fig. 7, the emissivity of  $H\alpha$  and  $D\alpha$  lines obtained from the simulation results shown in Figs. 3 and 6, respectively is plotted as a function of the distance from each limiter. In the case of GAMMA 10, data are extracted from the  $10 \leq r \leq 12$  cm and azimuthally averaged at the same  $z$ -position and those in Heliotron J are sampled at the position just above the limiter tip ( $Z \sim -17$  cm) and are plotted along the line of magnetic force.

In the case of Heliotron J, a point source of neutrals from the tip of the carbon limiter is given to simplify the simulation condition and three different density cases are presented. It is found that there is a steep decrease observed within 15 cm around the limiter tip and has no density dependence. In the region more than 20 cm away from the limiter tip, the decreasing rate of emissivity becomes weak and has the dependence that the decay length decreases with increasing density.

In the case of GAMMA 10, on the other hand, a noticeable reduction near the limiter is also observed but the decreasing rate is small compared with the Heliotron J at the same density. The decay length at the place more than 30 cm away from the limiter becomes longer and runs into 1 m. This tendency indicates that a large space between the plasma edge and the vacuum vessel enhances the particle transport along the axial direction in GAMMA 10. In the case of Heliotron J, however, particle transport in the SOL region is considered to be strongly prevented due to the twisted vacuum vessel wall.

## 5. Summary

Using three-dimensional Monte-Carlo code DEGAS ver.63, neutral transport simulation was successfully performed in the GAMMA 10 tandem mirror with open magnetic configuration and the Heliotron J with helical axis heliotron magnetic configuration, and the behavior of neutrals was investigated in detail based on the simulation results. The simulation results using 3-D mesh model including some inner components in the central-cell, such as the central midplane limiter and RF antenna, well explained 2-D image of visible light near the limiter captured with the medium-speed CCD camera. A mesh model of the carbon limiter was installed into the 3-D mesh structure modeling the Heliotron J vacuum vessel and plasma with non-axisymmetric configuration. 3-D simulation with assuming a particle source due to recycling on the limiter was performed and the neutral diffusion in radial and toroidal directions is investigated. The simulation with the particle source determined from the vertically viewing 2-D  $D\alpha$  image of the limiter also well reproduced 2-D image by the horizontally viewing CCD camera. Both simulation results showed that the neutral transport is significantly influenced by the geometry of the wall and plasma. From above these results, this analysis method using 3-D simulation is demonstrated in its validity and provides the important information for understanding of the plasma transport and confinement in helical configuration devices as well as open magnetic configuration devices.

## Acknowledgements

The authors would like to acknowledge the members of the Heliotron J supporting group and the GAMMA 10 group in the experiment. This work was performed with the support by the bidirectional collaboration research program (NIFS06KUHL010 and NIFS07KUGM024).

## References

- [1] D. Heifetz, D. Post, M. Petracic, et al., *J. Comput. Phys.* 46 (1982) 309.
- [2] D.P. Stotler et al., *Phys. Plasmas* 3 (1996) 4084.
- [3] Y. Nakashima, Y. Higashizono, et al., *J. Plasma Fus. Res.* 6 (2004) 546.
- [4] Y. Nakashima, Y. Higashizono, et al., *J. Nucl. Mater.* 337–339 (2005) 466.
- [5] M. Shoji et al., *J. Nucl. Mater.* 337–339 (2005) 186.
- [6] S. Kobayashi et al., in: *Proceedings of 31th EPS Conference on Plasma Physics*, London, 2004, 28G, P-5.097.
- [7] Y. Nakashima et al., *Contrib. Plasma Phys.* 48 (1–3) (2008) 141.
- [8] S.J. Zweben et al., *Phys. Plasmas* 9 (2002) 1981.
- [9] N. Nishino et al., *J. Nucl. Mater.* 337–339 (2005) 1073.
- [10] N. Nishino, Y. Nakashima, et al., *Plasma Fus. Res.* 1 (2006) 035.
- [11] M. Inutake et al., *Phys. Rev. Lett.* 55 (1985) 939.
- [12] F. Sano et al., *Nucl. Fus.* 45 (2005) 1557.
- [13] T. Mizuuchi et al., *Nucl. Fus.* 47 (2007) 395.